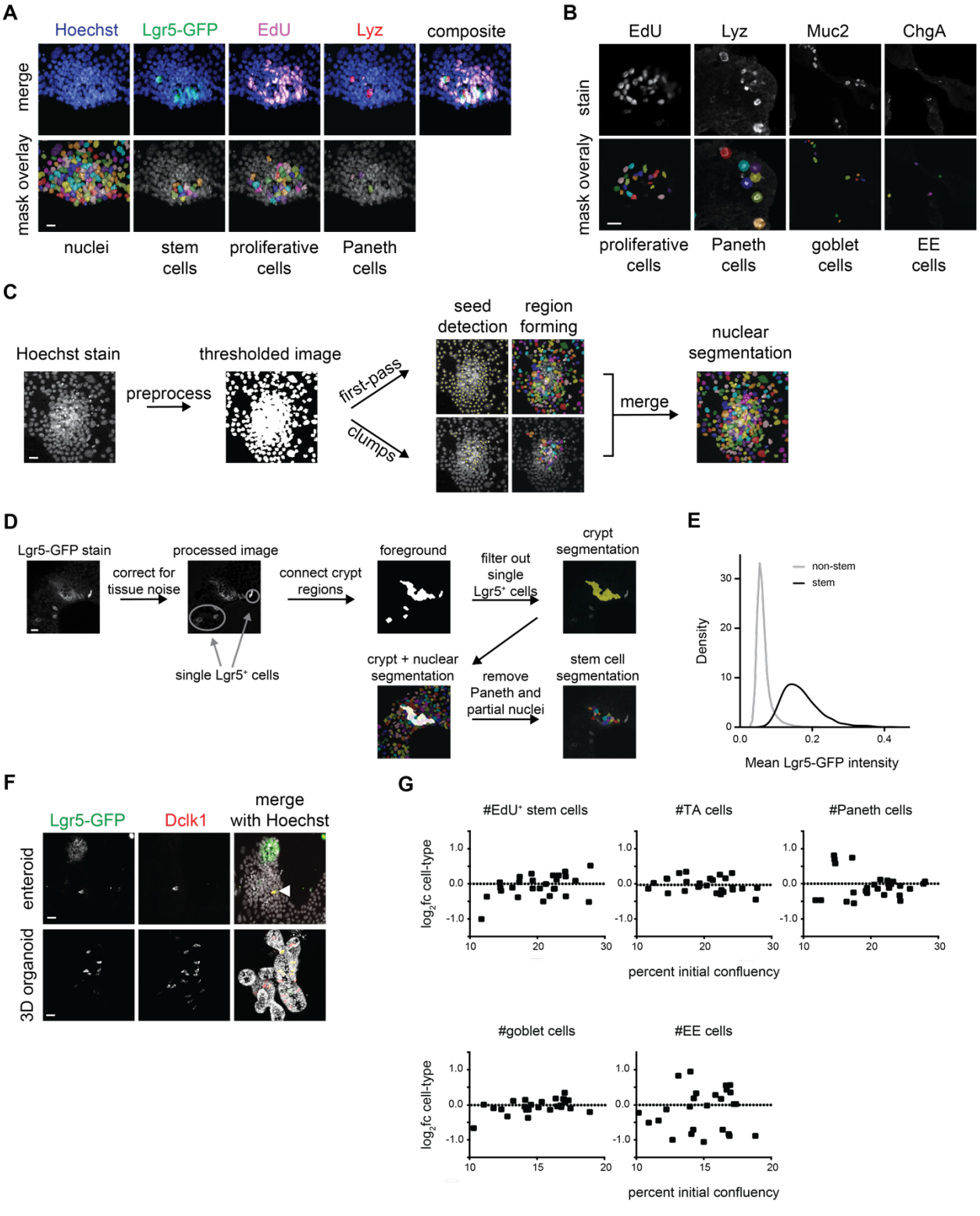
A
Hoechst
Lgr5-GFP
EdU
Lyz
composite
merge
mask overlay
nuclei
stem cells
proliferative cells
Paneth cells
B
EdU
Lyz
Muc2
ChgA
stain
mask overaly
proliferative cells
Paneth cells
goblet cells
EE cells
C
Hoechst stain
preprocess
thresholded image
first-pass
clumps
seed detection
region forming
merge
nuclear segmentation
D
Lgr5-GFP stain
correct for tissue noise
processed image
single Lgr5⁺ cells
connect crypt regions
foreground
filter out single Lgr5⁺ cells
crypt segmentation
crypt + nuclear segmentation
remove Paneth and partial nuclei
stem cell segmentation
E
non-stem
stem
Density
Mean Lgr5-GFP intensity
F
Lgr5-GFP
Dclk1
merge with Hoechst
enteroid
3D organoid
G
#EdU⁺ stem cells
#TA cells
#Paneth cells
log2fc cell-type
percent initial confluency
#goblet cells
#EE cells
log2fc cell-type
percent initial confluency

Figure S1. Related to Figure 1. Quantification of intestinal epithelial cell types in immunofluorescence images of enteroid monolayers.

(**A**) Example of crypt segmentation with pseudocolor overlay for each cell type readout. Scale bar 10μm.

(**B**) Example of segmentation of proliferating, Paneth, goblet, and enteroendocrine (EE) cells. Top: raw stain image for the indicated marker. Bottom: pseudocolor overlay of each identified cell type. Scale bar 10μm.

(**C**) Schematic of nuclear segmentation steps. Thresholded Hoechst stain images were segmented in two passes. The first pass segmented sparse nuclei and the second pass segmented clumped nuclei. Sparse and clumped segmentation were merged into the final nuclear segmentation. Yellow dots indicate identified markers of nuclear object locations, multi-pseudocolor overlay depicts individual nuclei segmented using a watershed algorithm. Scale bar 10μm.

(**D**) Schematic of stem cell segmentation. The Lgr5-GFP stain was first corrected for tissue noise and then thresholded. Size filtering was used to separate multi-cell membrane GFP regions (crypt regions) from single Lgr5-GFP^{+} cells. All nuclei in crypt regions (nuclei identified from Hoechst image segmentation of same region), with the exception of Paneth cell-associated nuclei, were counted as stem cells. Scale bar 10μm.

(**E**) Distribution of mean Lgr5-GFP intensity for segmented stem and non-stem cells. Mean intensity of max-projected Lgr5-GFP stain images was quantified in stem and non-stem cell nuclear segmentation regions. The distributions are well separated, indicating identification of distinct Lgr5^{+} stem cells and Lgr5^{-} non-stem cells.

(**F**) Single Lgr5-GFP^{+} cells are also Dclk1^{+} in enteroid monolayers (top; scale bar 10μm) and 3D organoids (bottom; scale bar 15μm) and are thus excluded from stem cell counts.

(**G**) Percent initial confluency was measured from brightfield images taken after crypt seeding and 48 hour cell type composition was quantified from immunofluorescence images. Y axis: log_2fc computed relative to the average of all wells. No relationship is observed between initial confluency and cell type frequencies.

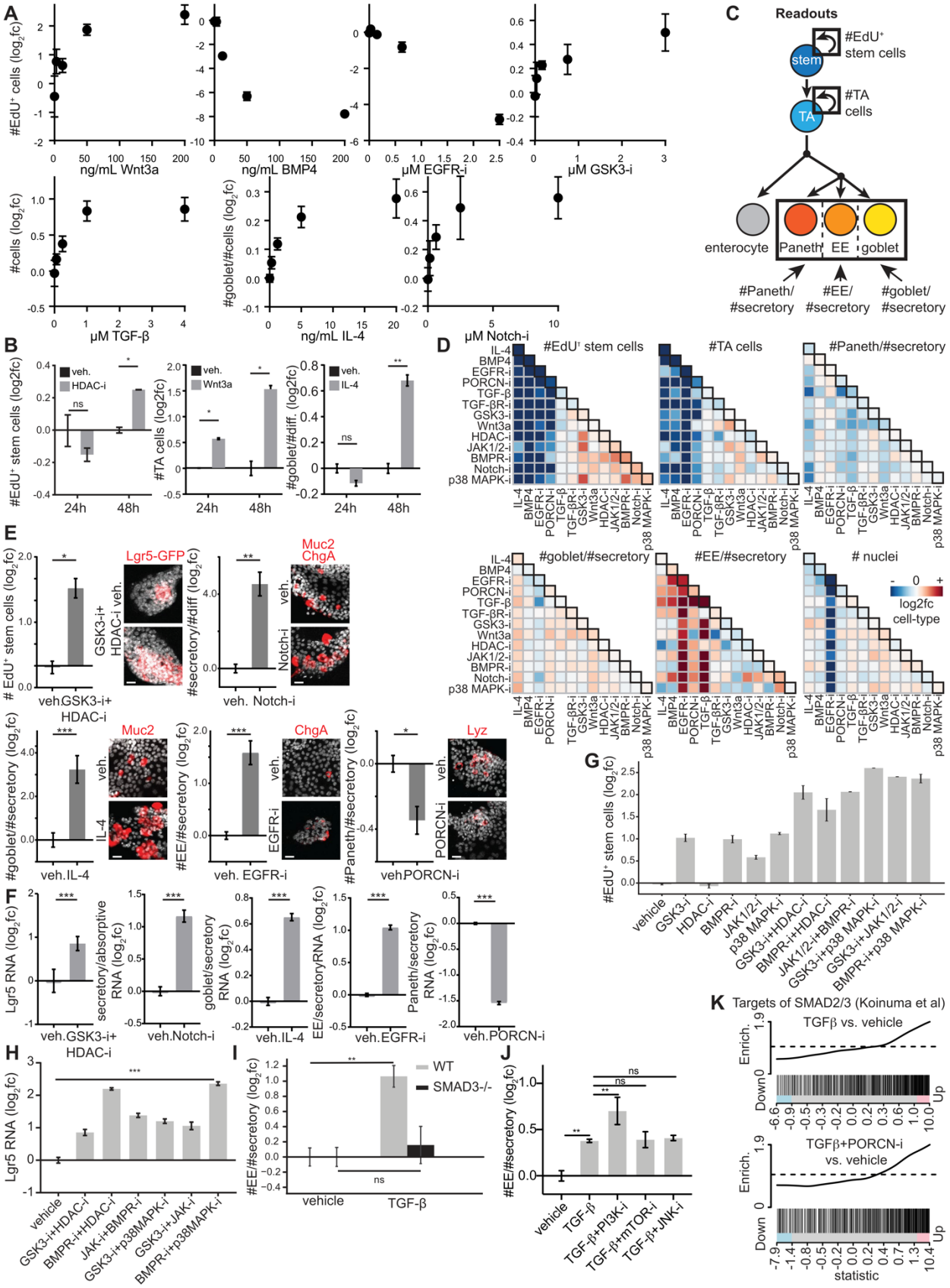
A
#EdU+ cells (log2fc)
ng/mL Wnt3a
ng/mL BMP4
μM EGFR-i
μM GSK3-i
#cells (log2fc)
μM TGF-β
#goblet/#cells (log2fc)
ng/mL IL-4
B
#EdU+ stem cells (log2fc)
veh.
HDAC-i
ns
24h
48h
Wnt3a
#TA cells (log2fc)
IL-4
#goblet/#diff. (log2fc)
C
Readouts
#EdU+ stem cells
stem
#TA cells
TA
enterocyte
Paneth
EE
goblet
#Paneth/ #secretory
#EE/ #secretory
#goblet/ #secretory
D
μM Notch-i
#EdU+ stem cells
#TA cells
#Paneth/#secretory
#goblet/#secretory
#EE/#secretory
nuclei
log2fc cell-type
IL-4
BMP4
EGFR-i
PORCN-i
TGF-β
TGF-βR-i
GSK3-i
Wnt3a
HDAC-i
JAK1/2-i
BMPR-i
Notch-i
p38 MAPK-i
E
EdU+ stem cells (log2fc)
Lgr5-GFP
GSK3-i+ HDAC-i
veh.
#secretory/#diff (log2fc)
Muc2
ChgA
Notch-i
#goblet/#secretory (log2fc)
IL-4
#EE/#secretory (log2fc)
EGFR-i
#Paneth/#secretory (log2fc)
PORCN-i
Lyz
F
Lgr5 RNA (log2fc)
secretory/absorptive RNA (log2fc)
goblet/secretory RNA (log2fc)
EE/secretoryRNA (log2fc)
Paneth/secretory RNA (log2fc)
G
#EdU+ stem cells (log2fc)
vehicle
GSK3-i
HDAC-i
BMPR-i
JAK1/2-i
p38 MAPK-i
GSK3-i+HDAC-i
BMPR-i+HDAC-i
JAK1/2-i+BMPR-i
GSK3-i+p38 MAPK-i
GSK3-i+JAK1/2-i
BMPR-i+p38 MAPK-i
H
Lgr5 RNA (log2fc)
GSK3-i+HDAC-i
BMPR-i+HDAC-i
JAK-i+BMPR-i
GSK3-i+p38MAPK-i
GSK3-i+JAK-i
BMPR-i+p38MAPK-i
I
#EE/#secretory (log2fc)
WT
SMAD3-/-
TGF-β
J
#EE/#secretory (log2fc)
TGF-β
TGF-β+PI3K-i
TGF-β+mTOR-i
TGF-β+JNK-i
K
Targets of SMAD2/3 (Koinuma et al)
TGFβ vs. vehicle
Enrich.
Down
Up
TGFβ+PORCN-i vs. vehicle
statistic

Figure S2. Related to Figure 2. Dose optimization, feature design, and benchmarking for combinatorial perturbation screen.

(**A**) Quantification of cell numbers and prevalence after perturbation with increasing doses of Wnt3a, BMP4, EGFR-i, GSK3-i, TGF-β, IL-4, or Notch-i. All data are represented as the $\log_2$ fold-change effect relative to control. Fraction of goblet cells was calculated as a percentage of all cells for comparison with previous studies. Concentration used for further studies are noted in Methods. n=4 (0μM, all conditions), 2 (Notch-i), or 3 (other conditions) wells.

Error bars mean +/- SEM.

(**B**) Quantification of cell type numbers for perturbations with known effects at 24 and 48 hours. n= 2 wells. Error bars mean +/- SEM.

(**C**) Schema of readouts. Proliferating progenitors: #EdU^+ stem or #TA cells. Secretory lineage: #goblet/#secretory, #Paneth/#secretory, or #EE/#secretory.

(**D**) Alternative visualizations of single and pairwise perturbation data. Quantification of progenitor readouts (#EdU^+ stem and #TA cells), secretory cell type readouts (#Paneth/#secretory, #goblet/#secretory, #EE/#secretory), and total cell number (# nuclei). Single perturbation effects are depicted along the diagonal (black boxes). n=28 (controls), 6-8 (single perturbations), or 2 (pairwise perturbations) wells.

(**E**) Enteroid monolayers respond as expected to modulators of stemness (GSK3-i + HDAC-i) and secretory cell prevalence (Notch-i, IL-4, EGFR-i, PORCN-i). Top: quantification of replicate wells. Bottom: representative images. Error bars mean +/- SEM. Scale bars 10μm. n=28 (vehicle), 4 (Notch-i), 8 (IL-4), 6 (EGFR-i), or 4 (PORCN-i) wells.

(**F**) Similar changes to (E) in cell type composition are observed at the RNA level. Enteroid monolayers were treated as indicated for 48 hours. Secretory/absorptive RNA= Atoh1/Hes1,

Paneth RNA=Lyz, goblet RNA=Muc2, EE RNA=ChgA, secretory RNA=Lyz+Muc2+ChgA. Error bars mean +/- SEM. Veh=vehicle. n=9 (vehicle, Lgr5), 6 (vehicle, all other markers) or 3 (all perturbations) wells.

(**G**) Single-compound controls for Lgr5 inducers in enteroid monolayers. Pairwise perturbations significantly increased ($p<0.05$) #EdU$^+$ stem cells compared to vehicle or either single perturbations (except BMPR-i + HDAC-i). Error bars mean +/- SEM. n=28 (control), 6 (GSK3-i, BMPR-i, JAK1/2-i), 8 (HDAC-i, p38 MAPK-i) or 2 (pairwise perturbations).

(**H**) Recapitulation of Lgr5$^+$ stem cell-inducing conditions by qRT-PCR in enteroid monolayers. Enteroid monolayers were treated as indicated for 48 hours. Pairwise perturbations significantly increased #EdU+ stem cells compared to vehicle. RNA levels were measured by qRT-PCR. Error bars mean +/- SEM. n=9 (vehicle) or 3 (perturbations) wells.

(**I**) SMAD3 deletion abrogates TGF-β-mediated induction of EE cells. Enteroid monolayers derived from SMAD3-/- mice were treated for 48 hours as indicated. Error bars mean +/- SEM. n=3 wells.

(**J**) Inhibitors of non-canonical TGF-β effectors do not abrogate TGF-β induction of EE cells in enteroid monolayers. 48 hour treatment. Error bars mean +/- SEM. n=3 wells.

(**K**) TGF-β and TGF-β + PORCN-i upregulate SMAD2/3 target genes in 3D organoids ($p=0.02$ for both TGF-β and TGF-β + PORCN-i vs. vehicle) (Methods).

* indicates p-values < 0.05; ** indicates p-values < 0.01; *** indicates p-values < 0.001; ns: not significant

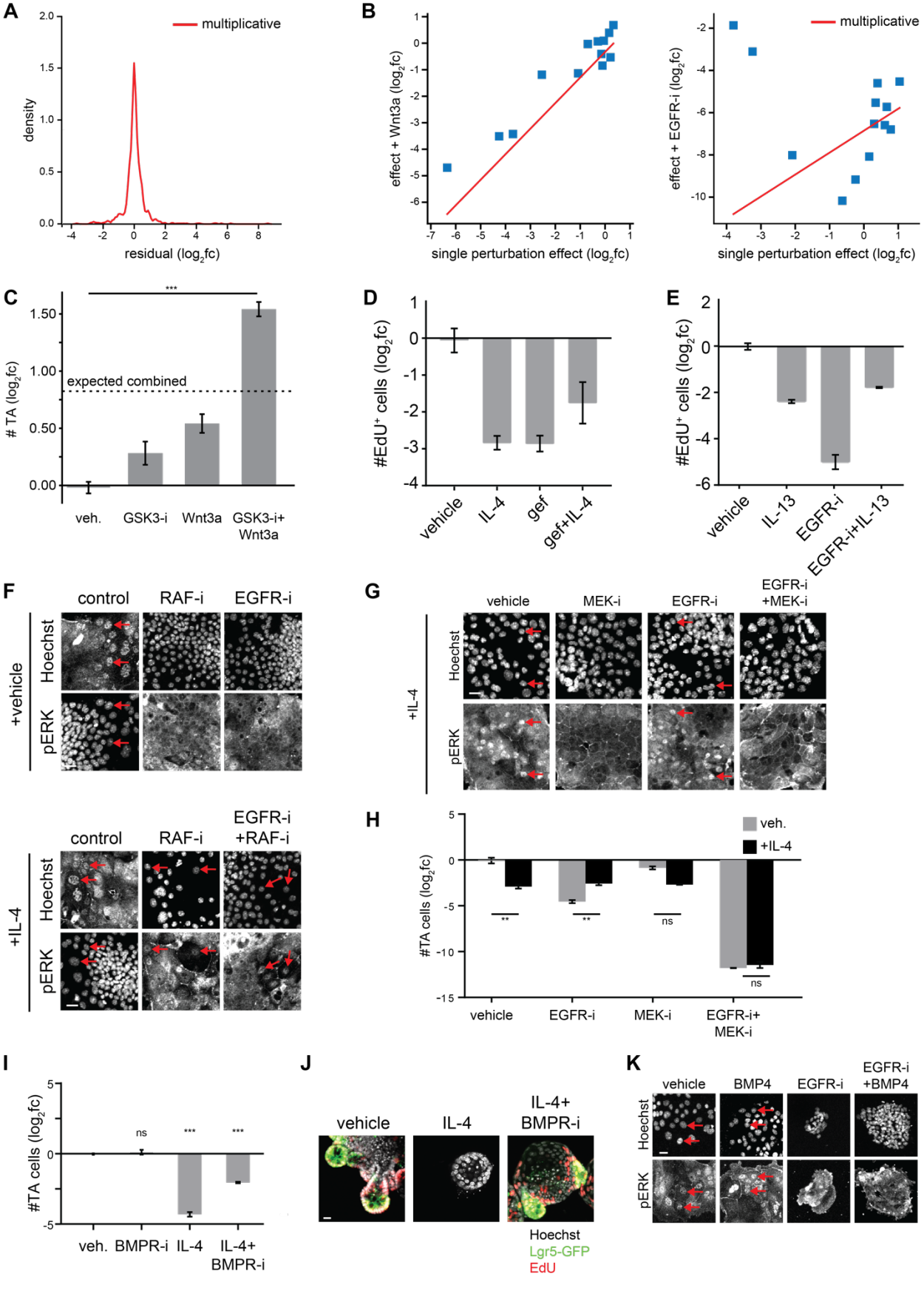
A
multiplicative
density
residual (log2fc)
B
effect + Wnt3a (log2fc)
single perturbation effect (log2fc)
multiplicative
effect + EGFR-i (log2fc)
single perturbation effect (log2fc)
C
TA (log2fc)
expected combined
***
veh.
GSK3-i
Wnt3a
GSK3-i+ Wnt3a
D
#EdU+ cells (log2fc)
vehicle
IL-4
gef
gef+IL-4
E
#EdU+ cells (log2fc)
vehicle
IL-13
EGFR-i
EGFR-i+IL-13
F
control
RAF-i
EGFR-i
+vehicle
Hoechst
pERK
control
RAF-i
EGFR-i +RAF-i
+IL-4
Hoechst
pERK
G
vehicle
MEK-i
EGFR-i
EGFR-i +MEK-i
+IL-4
Hoechst
pERK
H
#TA cells (log2fc)
veh.
+IL-4
**
**
ns
ns
vehicle
EGFR-i
MEK-i
EGFR-i+ MEK-i
I
#TA cells (log2fc)
ns
***
***
veh.
BMPR-i
IL-4
IL-4+ BMPR-i
J
vehicle
IL-4
IL-4+ BMPR-i
Hoechst
Lgr5-GFP
EdU
K
vehicle
BMP4
EGFR-i
EGFR-i +BMP4
Hoechst
pERK

Figure S3. Related to Figure 3. Evaluation of the multiplicative model and dissection of mutual antagonism between EGFR-i and IL-4.

(**A**) Perturbation effects are generally similar to the predictions of the multiplicative model. Distribution of residual between predicted and observed values across all cell type readouts is shown.

(**B**) Examples of well-predicted (Wnt3a) and divergent (EGFR-i) perturbations are shown. Effects shown are on #TA cells.

(**C**) The combination effect of Wnt3a and GSK3-i is much higher (effect size > 2, $p<0.01$) than would be expected under the multiplicative model (dashed line). Error bars mean +/- SEM. n=28 (vehicle), 6 (GSK3-i and Wnt3a), or 2 (Wnt3a + GSK3-i) wells.

(**D**) EGFR inhibitor gefitinib (gef) antagonizes the effect of IL-4 on #EdU^+ cells. Error bars mean +/- SEM. n=2 for all conditions.

(**E**) IL-13, a closely related cytokine to IL-4, antagonizes the effect of EGFR-i on #EdU^+ cells. Error bars mean +/- SEM. n=2 for all conditions.

(**F**) IL-4 bypasses RAF-i to activate ERK signaling. Enteroid monolayers were treated with the indicated compounds for 48 hours and then stained for phospho-Erk1/2. Top: Both RAF-i and EGFR-i treatment inhibit Erk activation. Bottom: Co-treatment of IL-4 with either RAF-i or RAF-i + EGFR-i rescues Erk activation (nuclear translocation of phospho-Erk). Red arrows indicate example cells with nuclear phospho-Erk. Scale bars 5μm.

(**G**) MEK inhibition reduces Erk activation even in the context of IL-4 treatment. Enteroid monolayers were treated with the indicated compounds for 24 hours and then stained for phospho-Erk1/2. Red arrows indicate example cells with nuclear phospho-Erk. Scale bar 7.5μm.

(**H**) Antagonistic effect of IL-4 on EGFR-i is dependent on MEK activity. Enteroid monolayers were treated as indicated for 48 hours and the number of TA cells were quantified. Error bars mean +/- SEM. n=2 (vehicle and MEK-i) or 3 (all other perturbations) wells.

(**I**) BMP receptor inhibition (BMPR-i) blocks IL-4-induced downregulation of TA cell numbers and stem cell numbers. Enteroid monolayers were treated as indicated for 48 hours and both EdU^+ stem and TA cell numbers quantified. All comparisons are to vehicle condition. Error bars mean +/- SEM. n=28 (vehicle), 6 (BMPR-i and IL-4), or 2 (IL-4 + BMPR-i) wells.

(**J**) BMP receptor inhibition blocks IL-4-induced downregulation of proliferation and stemness in 3D organoids. 3D organoids were treated with vehicle or IL-4 in the presence and absence of BMP receptor inhibitor for 48 hours and then stained for proliferating cells (EdU^+) and stem cells ($Lgr5^+$). Scale bar 7.5μm.

(**K**) BMP4 has no effect on Erk signaling. Enteroid monolayers were treated as indicated for 48 hours and then stained for phospho-Erk1/2. Red arrows indicate example cells with nuclear phospho-Erk. Scale bars 5μm.

* indicates p-values < 0.05; *** indicates p-values < 0.001; ns: not significant

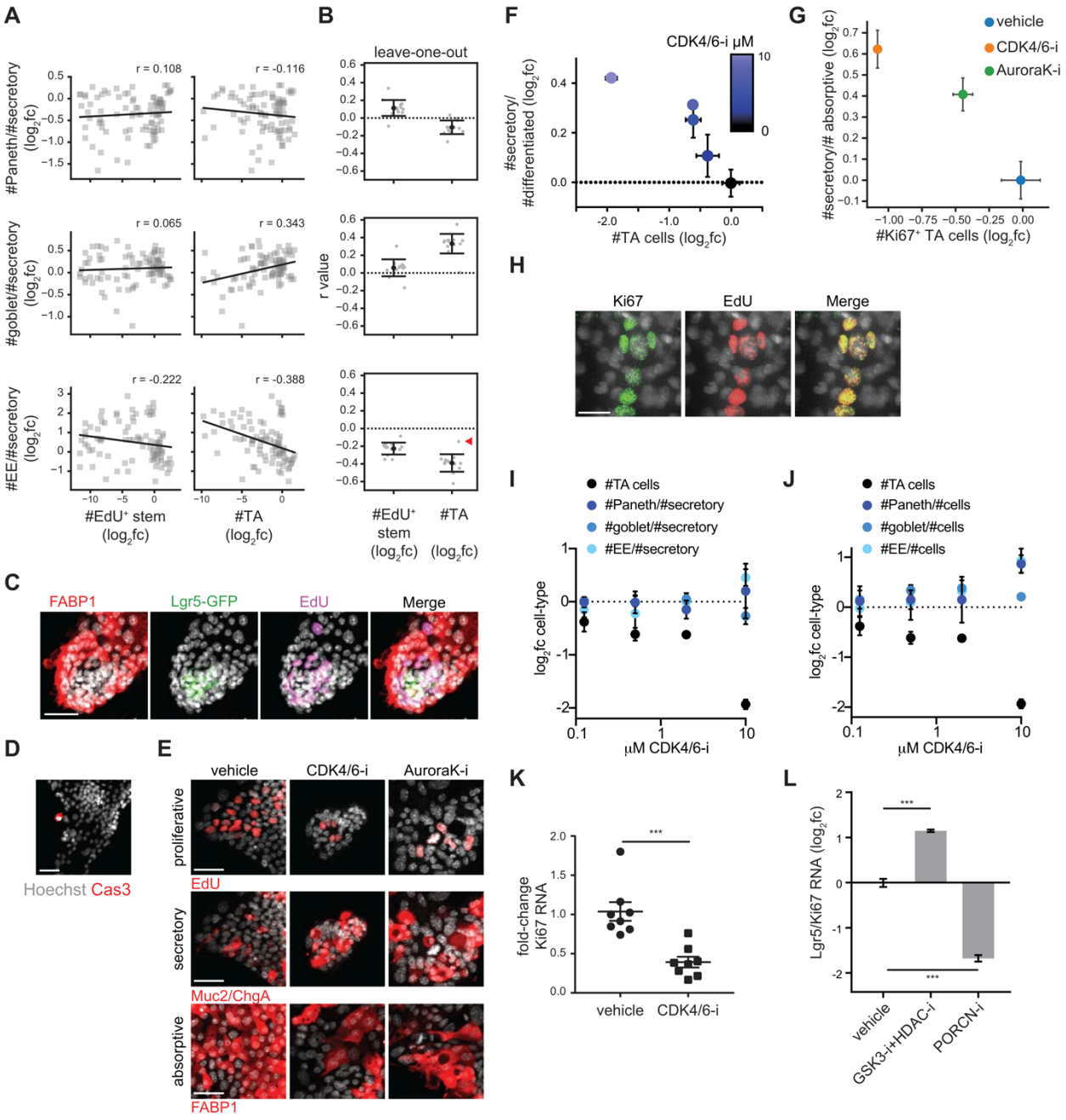

Figure S4. Related to Figure 4. Modulating TA cell proliferation causes an anti-correlated change in secretory cell prevalence.

(**A**) Numbers of TA cells anti-correlate with EE cell fractions. Perturbation effects (log_2fc) are plotted pairwise for each feature. Correlation coefficient (r) as indicated.

(**B**) Each of 13 perturbations was individually dropped from the dataset and correlation coefficients (r value) were calculated. Red arrowhead indicates loss of correlation between #TA cells and #EE/#secretory after dropping EGFR-i. Error bars mean +/- SD.

(**C**) Enterocytes (FABP1) surround crypts, and do not colocalize with proliferative (EdU^+) cells. Enteroid monolayers were cultured for 48 hours and then stained with indicated cell type markers. Scale bar 40 μm.

(**D**) Few apoptotic cells are visualized in enteroid monolayers. Enteroid monolayers were cultured for 48 hours and then stained with Active-Caspase3 to visualize apoptotic cells. Scale bar 40 μm.

(**E**) Effect of cell cycle inhibitors on the number of proliferative, secretory, and absorptive cells. Enteroid monolayers were treated as indicated for 48 hours, and then proliferative (EdU^+) cells, secretory ($Muc2^+$ and $ChgA^+$) cells, and absorptive ($FABP1^+$) cells were visualized. Representative images are depicted. Scale bar 40 μm.

(**F**) CDK4/6-i (palbociclib) increased the secretory cell fraction and decreased TA cell numbers in a dose-dependent manner. Increasing concentrations of CDK4/6-i were applied (concentrations indicated by color bar) to enteroid monolayers for 48 hours. Changes in the TA cells (#TA cells log_2fc) and secretory cell prevalence amongst differentiated cells (#secretory/#differentiated log_2fc) were quantified. The color of each point indicates the concentration of CDK4/6-i applied. Error bars mean +/- SEM. n=4 (0 μM CDK4/6-i) or 2 (all other concentrations) wells.

(**G**) Inhibiting cell cycle progression increases secretory cell fractions. Enteroids were treated as indicated for 48 hours, after which #$Ki67^+$ TA cells, and #secretory/#absorptive cells were quantified. n = 3 wells. Error bars mean +/- SEM.

(**H**) Proliferative cells visualized by either Ki67 or EdU colocalize. Enteroid monolayers were cultured for 48 hours and then stained with Ki67 or EdU to visualize proliferative cells. Scale bar 20 μm.

(**I-J**) Effect of CDK4/6-i on individual cell type features over a range of doses. Error bars mean +/- SEM. n=4 (0 μM CDK4/6-i) or 2 (all other concentrations) wells.

(**K**) Small intestinal epithelial crypts were harvested from mice treated with vehicle or CDK4/6-i (palbociclib). To quantify changes in proliferation, Ki67 RNA was measured by qRT-PCR. n=8 wells. Error bars mean +/- SEM.

(**L**) 3D organoids were treated with GSK3-i + HDAC-i for 48 hours or PORCN-i for 24 hours and the stem (Lgr5) to proliferating (Ki67) RNA ratio was measured by qRT-PCR to confirm enrichment. n=3 wells. Error bars mean +/- SEM.

*** indicates p-values < 0.001

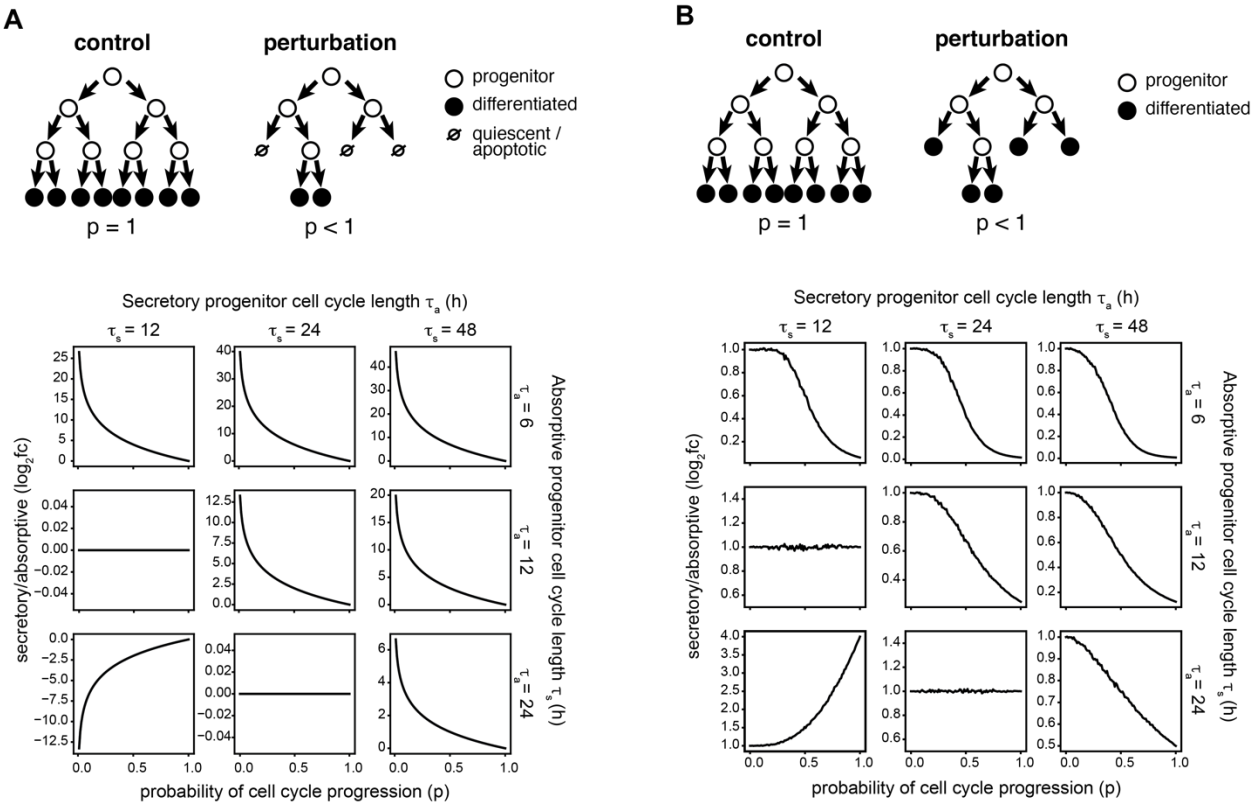

Figure S5. Related to Figure 5. Cell cycle modulators affect the secretory to absorptive ratio due to differential amplification of secretory and absorptive progenitors.

(**A**) Diagram and output of quiescence probability model (Model 0).

(**B**) Diagram and output for the stochastic model in which TA cells differentiate upon quiescence (10000 runs, Model 2).

Model and parameters described in Methods.

Cell type	**Marker**	**Precision**	**Recall**	**F1 Score**
nuclei	Hoechst	0.9965	0.9936	0.9951
goblet cells	Muc2	1	0.8998	0.9473
EE cells	ChgA	0.8551	0.9248	0.8886
Paneth cells	Lyz	0.9018	0.9642	0.9319
EdU^+ cells	EdU	1	0.9557	0.9774
crypt regions	Lgr5-GFP	0.9816	0.9877	0.9846
stem cells	Lgr5-GFP	0.9724	0.9756	0.9740
$Lgr5^+/Dclk1^+$ cells	Lgr5-GFP	0.8208	0.9087	0.8625

Table S1. Related to STAR Methods. Evaluation of the performance of cell type identification algorithms.

Cell Type	***In Vivo* (%)**	**Enteroid Monolayer (% of all cells)**
Paneth	7.5% of crypt cells(Cheng and Leblond, 1974b)	3.1
Goblet	4-6% (Cheng and Leblond, 1974b)	3.8
EE	0.6% (Cheng and Leblond, 1974b)	0.4
Enterocyte	86% (Cheng and Leblond, 1974b)	63.3

Table S2. Related to Figure 1. Comparison of enteroid monolayer cell type composition with literature reports of small intestine cell type composition. Measurements are presented as percentage of all cells for comparison with literature values.

Cell Type	Enteroid Monolayer (%)
Paneth	1.5
Goblet	6.1
EE	3.0
Enterocyte	5.0

Table S3. Related to Figure 1. Enteroid monolayer differentiated cell type composition after culture establishment (4 hours after seeding).

Pathway	Perturbation	Target	Designation	Pathway Effect	Published Effect(s) on Intestinal Epithelium	Dose Ref.
EGFR	erlotinib	EGFR	EGFR-i	inhibit	Reduced proliferation, increased EE cell (Basak et al., 2017)	(Basak et al., 2017a)
Wnt	Wnt3a	Frizzled	Wnt3a	activate	Increased proliferation (Clevers, 2013)	(Thorne et al., 2018)
	IWP-2	PORCN	PORCN-i	inhibit	Decreased proliferation, stem cells, Paneth cells (Basak et al., 2017; van Es et al., 2005; Farin et al., 2016; Rodríguez-Colman et al., 2017)	(Yin et al., 2014)
	CHIR99021	GSK3	GSK3-i	activate	Increased proliferation, stem cells (Yin et al., 2014)	(Yin et al., 2014)
BMP	BMP4	BMPR	BMP4	activate	Decreased proliferation and stem cells (Qi et al., 2017)	(Thorne et al., 2018)
	LDN-193189	ALK2/3	BMPR-i	inhibit	Increased proliferation and stem cells (Li et al., 2018)	(Thorne et al., 2018)
TGF-β	TGF-β	TGF-βR	TGF-β	activate	Important for differentiation *in vivo* *(Flentjar et al., 2007; van der Flier et al., 2009; Li et al., 2018)*	(Han et al., 2014)
	EW-7197	ALK4/5	TGF-βR-i	inhibit	?	(Hong et al., 2017)
Notch	DAPT	γ-secretase	Notch-i	inhibit	Increased secretory cell types (VanDussen et al., 2012)	(Yin et al., 2014)
IL-4-JAK	IL-4	IL-4R	IL-4	activate	Increased goblet cells (von Moltke et al., 2015)	(von Moltke et al., 2015)
	baricitinib	JAK1/2	JAK1/2-i	inhibit	Altered stem cell numbers (Batlle et al., 2002; Richmond et al., 2018)	(Dames et al., 2015)
HDAC	valproic acid	HDAC1/2	HDAC-i	inhibit	Increased stem cells (von Moltke et al., 2015; Yin et al., 2014)	(Yin et al., 2014)
p38 MAPK	SB202190	p38 MAPK	p38 MAPK-i	inhibit	Increased proliferation (Houde et al., 2001; Sato et al., 2011)	(Sato et al., 2011)

Table S4. Related to Figure 2. Selection of cell type perturbations for study. For each perturbation, the specific pathway and target are indicated, as is the expected effect on the pathway and tissue. Designation is the code with which the perturbation is referred to in figures and text.

	Downregulating		Upregulating	
	Perturbation	**Log_2fc**	**Perturbation**	**Log_2fc**
EdU^+ stem number	BMP4 + JAK1/2-i	-11.380	GSK3-i + p38 MAPK-i	2.602
	BMP4	-11.080	GSK3-i + JAK1/2-i	2.405
	BMP4 + Wnt3a	-10.380	BMPR-i + p38 MAPK-i	2.363
TA number	EGFR-i + HDAC-i	-9.476	GSK3-i + Wnt3a	1.541
	IL-4 + PORCN-i	-9.437	GSK3-i + JAK1/2-i	1.415
	EGFR-i + TGF-βR-i	-8.512	BMPR-i + Wnt3a	1.240
Secretory fraction (of differentiated cells)	TGFβ + Wnt3a	-1.544	GSK3-i + EGFR-i	1.109
	BMP4 + TGFβ	-1.509	EGFR-i + BMPR-i	1.096
	TGFβ + HDAC-i	-1.452	EGFR-i + JAK1/2-i	1.062
Paneth fraction (of secretory cells)	IL-4 + TGF-β	-1.651	BMPR-i + HDAC-i	0.307
	PORCN-i + TGF-β	-1.466	GSK3-i + HDAC-i	0.305
	IL-4 + p38 MAPK-i	-1.417	EGFR-i + TGF-β	0.270
Goblet fraction (of secretory cells)	EGFR-i + TGF-β	-1.209	IL-4 + p38 MAPK-i	0.724
	Notch-i + EGFR-i	-0.880	TGF-βR-i + Wnt3a	0.611
	EGFR-i + PORCN-i	-0.558	IL-4 + TGF-β	0.604
EE fraction (of secretory cells)	TGF-βR-i + Wnt3a	-1.525	PORCN-i + TGF-β	2.885
	IL-4 + HDAC-i	-1.419	Notch-i + TGF-β	2.542
	GSK3-i + HDAC-i	-1.098	TGF-β	2.282

Table S5. Related to Figure 2. Top perturbations in modulating cell type composition.